Electronic Supplementary Information

Impact of Molecular Orientations on the Energy Levels of A-D-A Acceptors: Implication for the Charge Separation Driving Force of Organic Solar Cells

Miaofei Huang, [a,b] Guangchao Han [a] and Yuanping Yi [*a,b]

[a] Beijing National Laboratory for Molecular Sciences, CAS Key Laboratory of Organic Solids, Institute of Chemistry, Chinese Academy of Sciences, Beijing 100190, China.

[b] School of Chemical Sciences, University of Chinese Academy Sciences, Beijing 100049, China.

*E-mail: ypyi@iccas.ac.cn

COMPUTATIONAL METHODS

Optimization of Crystal Structures

Both IDIC-4F and INIC-4F crystals were optimized by VASP while the cell parameters were kept at the experimental values. The electronic structure and ion-electron interactions were calculated using the Perdew-Burke–Ernzerhof (PBE) functional and projector augmented wave (PAW) pseudopotentials. All geometry optimizations were performed in a plane-wave basis set with an energy cut-off of 450 eV and a Gaussian smearing of 0 eV. The Brillouin zones were sampled with 3 × 2 × 1 and 2×2×1 Monkhorst-Pack mesh k-point grids[1] for IDIC-4F and INIC-4F, respectively. The geometries were optimized using a conjugated gradient algorithm and all the atoms were fully relaxed. In the density functional theory (DFT) calculations, the total energy in the self-consistent field method and the force converged up to 10^{-5} eV and 0.02 eV/Å, respectively. Besides, the optimized Y6 crystal was obtained from the crystal structure published by Zhu et al.[2]

Calculations of Energy Levels in the Gas and the Solid Phase.

In addition to ionization potential (IP) and electron affinity (EA), the fundamental transport gap (E_g^t) was also calculated, which is the difference between IP (IP = $E_+ - E_0$) and EA (EA = $E_0 - E_-$), E_g^t = IP − EA; here E_0, E_+, and E_- denote the total potential energies of the ground state (S_0) and the cationic and anionic states, respectively. The DFT was used to calculate the S_0 and ionic states of molecules at the ωB97X-D/def2-SVP level. To obtain a more reliable description of the electronic properties, the range separation parameter ω was optimized by the gap tuning procedure with minimizing the value of J^2,

$$J^2 = \sum_{i=0}^{1} [\varepsilon_H(N+i) + IP(N+i)]^2 \quad (1)$$

where ε_H denotes the highest occupied molecular orbital (HOMO) energy of the molecule; N is the number of electrons.

In the calculations of crystals, isolated molecules were extracted directly from the optimized crystals and calculated for the gas phase data. In solid, self-consistent quantum mechanics/embedded charge (sc-QM/EC) calculations were performed for clusters extracted from optimized crystals to obtain the solid data. In the first QM/EC calculation, the central molecule is addressed at the DFT level and the atomic charges of the cluster are initialized according to the DFT calculations on isolated molecules. Merz-Singh-Kollman[3] scheme is used to replicate the electrostatic potential derived from QM/EC for the atomic charge of the central molecule. Afterward, each molecule in the polarizable region is treated as a QM component with the atomic point charges

of other molecules, which are updated from previous QM/EC operation results, and the process is iterative. Through the QM/EC single-point iterative computations, the atomic charges of the center and ambient molecules are redistributed and thus can explicitly account for the effects of charge polarization. The workflow is finished until the total energy difference between the two adjacent QM/EC calculations of the central molecule is less than 10^{-5} Hartree.

In the sc-QM/EC calculation, different cluster models were used to matching different solid environments of the central molecule (**Figure S1**). The spherical cluster model serves for obtaining the bulk phase molecule data; The hemispherical cluster model serves for obtaining the surface molecule data. The model of gradually piled layers on the surface of the central molecule in units of crystal cells illustrates the movement of the central molecule (or carrier) from the surface to the bulk phase. All cluster radii were set to 100 Å, and according to the related reference[4] and our test, the polarization radius of 50 Å (**Figure S2**), i.e., only molecules within 50 Å of the central molecule participate in the self-consistent process, was chosen in all systems to reduce computational cost. In addition, in order to investigate the structure-property relationship, the geometries of the three molecules were optimized at the B3LYP/def2-SVP level (all alkyl side chains were replaced by methyl groups to simplify the calculation). Then, the molecular polarity properties, including dipole moment μ, end-group fragment dipole moment μ_{EG}, half molecular dipole moment μ_{HalfM} (all in Debye), their traceless quadrupole moment $|\Theta|$ in Debye•Å^{-1}, and electrostatic potential, are calculated and analyzed at the tuned ωB97X-D/def2-SVP level. Further, to test the influence of different basis sets, taking Y6 as an example, we have calculated the molecular IP and EA by using the def2-SVP, def2-TZVP, and def2-TZVPP basis sets and the tuned-ωB97X-D functional in combination with the polarizable continuum model (the dielectric constant is set to 5.0). As shown in **Figure S3**, the def2-SVP basis set can achieve sufficient accuracy for evaluating the IP and EA (the difference is within 0.1 eV compared with the converged results). All these calculations were performed by Gaussian 16 package.[5] The molecular polarity properties are analyzed by the Multiwfn program.[6]

REFERENCES

1. H. J. Monkhorst and J. D. Pack, Special points for Brillouin-zone integrations, *Phys. Rev. B*, 1976, **13**, 5188-5192.
2. L. Zhu, J. Zhang, Y. Guo, C. Yang, Y. Yi and Z. Wei, Small exciton binding energies enabling direct charge photogeneration towards low-driving-force organic solar cells, *Angew. Chem. Int. Ed.*, 2021, **60**, 15348-15353.
3. U. C. Singh and K. P. A., An approach to computing electrostatic charges for molecules, *J. Comput. Chem.*, 1984, **5**, 129-145.

4. L. Zhu, Z. Tu, Y. Yi and Z. Wei, Achieving small exciton binding energies in small molecule acceptors for organic solar cells: effect of molecular packing, *J. Phys. Chem. Lett.*, 2019, **10**, 4888-4894.
5. M. J. Frisch, G. W. Trucks, H. B. Schlegel, G. E. Scuseria, M. A. Robb, J. R. Cheeseman, G. Scalmani, V. Barone, G. A. Petersson, H. Nakatsuji, X. Li, M. Caricato, A. V. Marenich, J. Bloino, B. G. Janesko, R. Gomperts, B. Mennucci, H. P. Hratchian, J. V. Ortiz, A. F. Izmaylov, J. L. Sonnenberg, Williams, F. Ding, F. Lipparini, F. Egidi, J. Goings, B. Peng, A. Petrone, T. Henderson, D. Ranasinghe, V. G. Zakrzewski, J. Gao, N. Rega, G. Zheng, W. Liang, M. Hada, M. Ehara, K. Toyota, R. Fukuda, J. Hasegawa, M. Ishida, T. Nakajima, Y. Honda, O. Kitao, H. Nakai, T. Vreven, K. Throssell, J. A. Montgomery Jr., J. E. Peralta, F. Ogliaro, M. J. Bearpark, J. J. Heyd, E. N. Brothers, K. N. Kudin, V. N. Staroverov, T. A. Keith, R. Kobayashi, J. Normand, K. Raghavachari, A. P. Rendell, J. C. Burant, S. S. Iyengar, J. Tomasi, M. Cossi, J. M. Millam, M. Klene, C. Adamo, R. Cammi, J. W. Ochterski, R. L. Martin, K. Morokuma, O. Farkas, J. B. Foresman and D. J. Fox *Gaussian 16 Rev. A.03*, Gaussian, Inc., Wallingford, CT, 2016.
6. T. Lu and F. W. Chen, Multiwfn: a multifunctional wavefunction analyzer, *J. Comput. Chem.*, 2012, **33**, 580-592.

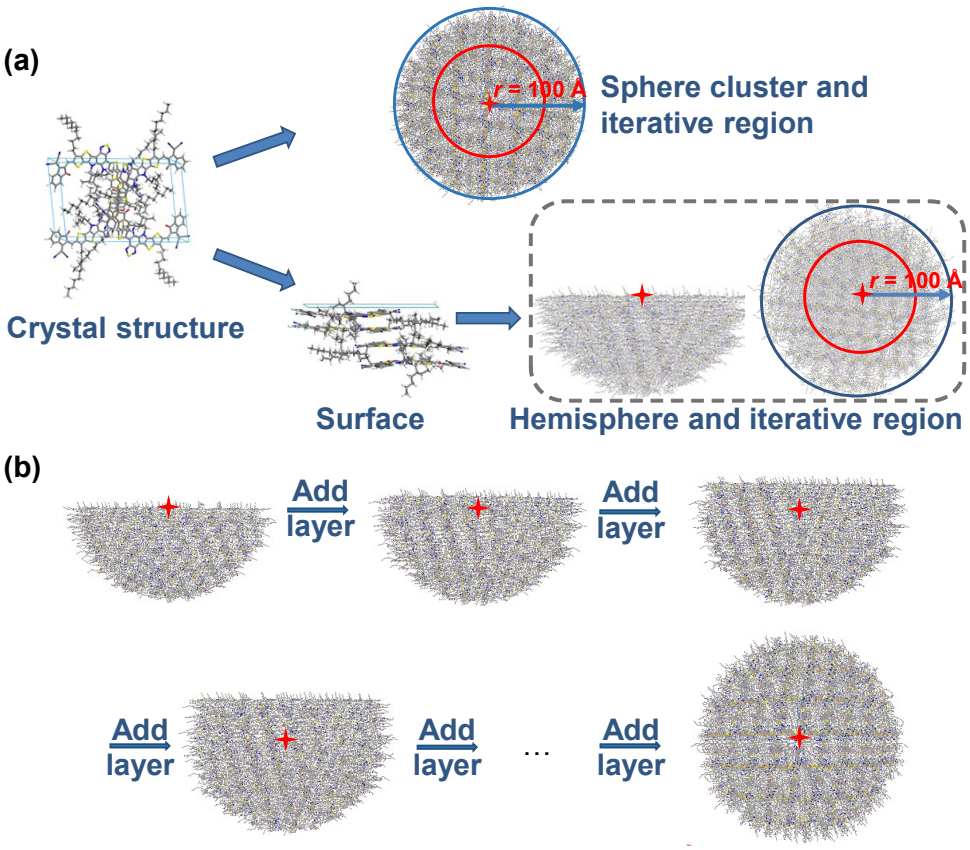

Figure S1. (a) The spherical cluster model and the hemispherical cluster model correspond to the bulk molecule and the surface molecule respectively for sc-QM/EC calculation. Two-level scheme for the cutoff of molecular clusters is also presented. (b) Evolution of cluster model which represents the process of carrier moving from surface to bulk phase.

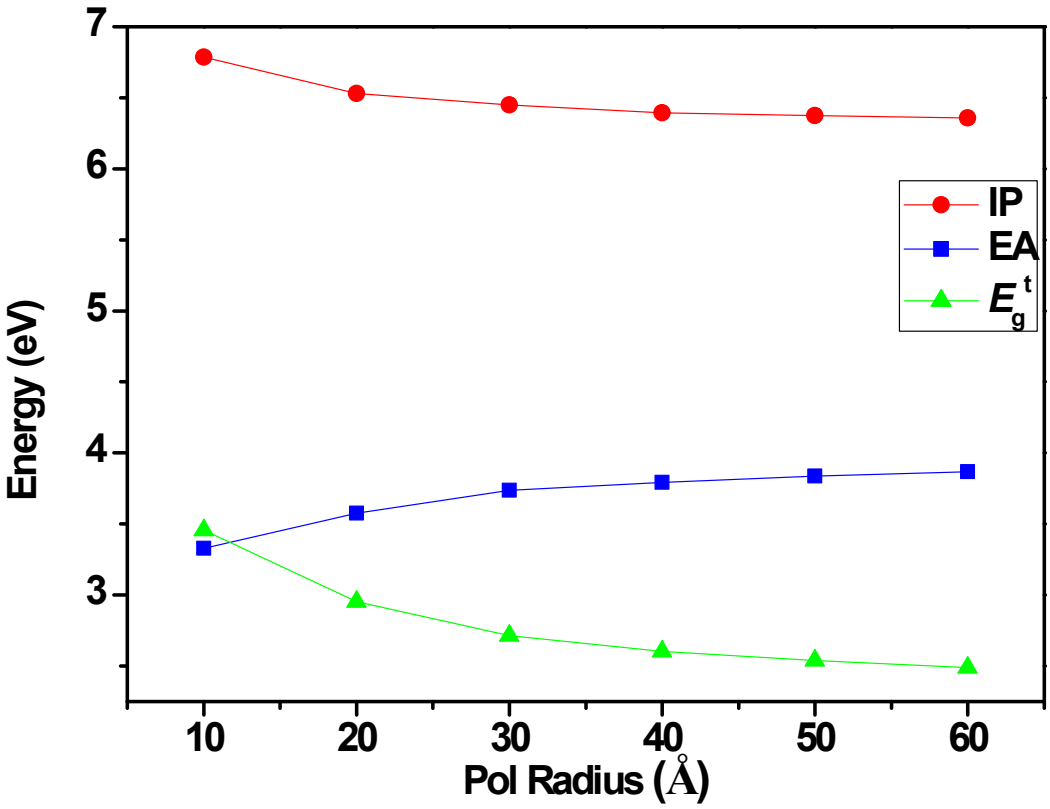

Figure S2. Dependence of the IP, EA, and E_g^t on the radius of the polarizable region (calculated at the tuned-ωB97X-D/def2-SVP level), taking the 10-1 surface of Y6 crystal as an example.

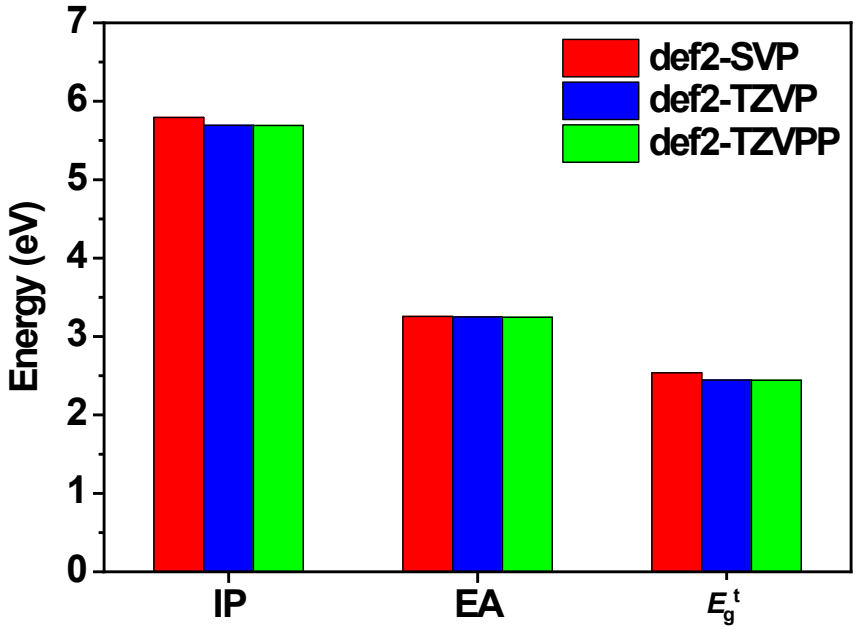

Figure S3. IP, EA, and E_g^t calculated by using the def2-SVP, def2-TZVP, and def2-TZVPP basis sets and the tuned-ωB97X-D functional in combination with the polarizable continuum model for the Y6 molecule.

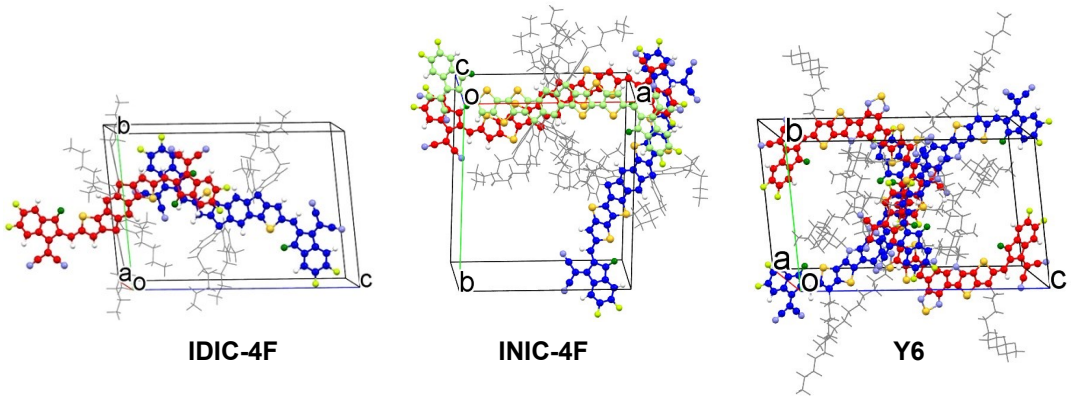

Figure S4. Optimized crystal structures of the studied nonfullerene small-molecule acceptors without changing the lattice parameters. The lattice parameters are listed as follows, IDIC-4F: a = 7.97 Å, b = 18.14 Å, c = 25.43 Å, α = 97.75°, β = 91.74°, γ = 99.42°; INIC-4F: a = 19.91 Å, b = 22.27 Å, c = 26.75 Å, α = 82.01°, β = 83.38°, γ = 89.82°; Y6: a = 14.53 Å, b = 19.80 Å, c = 28.53 Å, α = 95.14°, β = 101.46°, γ = 107.36°.

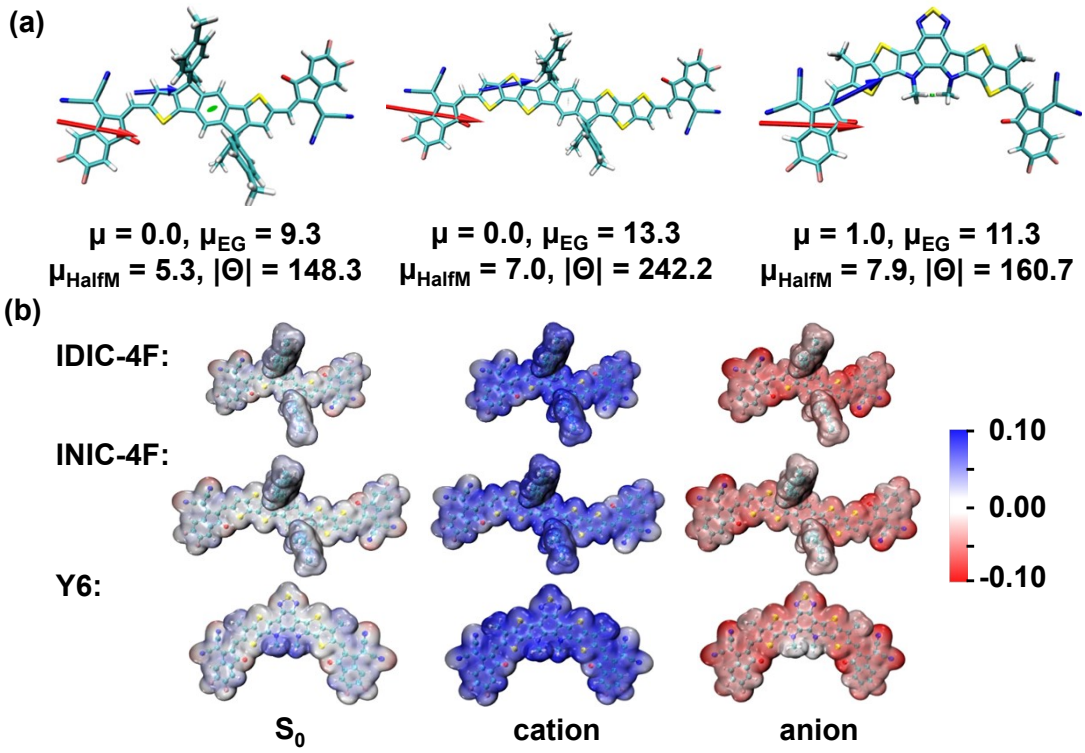

Figure S5. (a) Molecular geometries of IDIC-4F, INIC-4F, and Y6 optimized at the B3LYP/def2-SVP level, and their molecular μ (green arrows), μ_{EG} (red arrows), μ_{HalfM} (blue arrows) (all in Debye), and |Θ| in Debye•Å^{-1} calculated at the tuned ωB97X-D/def2SVP level. All of the alkyl groups are replaced by methyl groups. (b) Electrostatic potentials of S_0 and the cationic and anionic states of the optimized molecules in the gas phase.